Observation of Shot Noise in Phosphorescent Organic Light-Emitting Diodes

Thaddee Kamdem Djidjou, Dieter Alexander Bevans, Sergey Li, and Andrey Rogachev

***Abstract*— We employed a cross correlation method to study current noise in phosphorescent organic light-emitting diodes. The noise spectra revealed two frequency-dependent components. The first component displays $1/f^{1.3}$ dependence and correlates with the light emission of the devices. The second component is dominant in low-bias regime and varies as $1/f^{2.8}$. It is attributed to inhomogeneities of the barrier height at metal/organic interface. The extended bandwidth of the method allowed us to resolve frequency-independent term in the noise power, which was dominated by the shot noise. At bias voltages from 2.4 to 2.5 V, the Fano factor characterizing shot noise is close to one, confirming that the electron transport in this regime is limited by the carrier injection across metal/organic interface. At higher biases, in the regime where the transport is bulk-limited, the Fano factors drops to 0.5. Possible physical reasons for such behavior are discussed.**

***Index Terms*— Fano factor, low-frequency noise, noise generators, organic light-emitting diode (OLED), shot noise.**

I. Introduction

ORGANIC light-emitting diodes (OLEDs), field-effect transistors (FETs), and organic solar cells (OSCs) are important alternatives to traditional inorganic electronic devices in low-cost large-area applications [1], [2]. The OLEDs are already used in display manufacturing; the efficiency of OSC as high as 10% has been reported [2]. In addition, there is a strong progress in OLED-based sensors for chemical and biological applications [3].

To make the organic devices more competitive, their efficiency and reliability need to be improved [4]. A modern organic device, for example an OLED, is comprised of several layers introduced to improve and balance the carrier injection. In a typical industrial setting, the nondestructive characterization of an OLED is limited by measurements of its emission spectrum, electrical current, electroluminescence, and efficiency. All these measurements are carried out at a constant dc bias and certainly are not sufficient to fully characterize a real multilayer OLED.

Manuscript received April 17, 2014; revised June 18, 2014; accepted June 20, 2014. Date of publication July 29, 2014; date of current version August 19, 2014. This work was supported by the National Science Foundation CAREER under Grant DMR 0955484. The review of this paper was arranged by Editor Z. Celik-Butler.

T. K. Djidjou, D. A. Bevans, and A. Rogachev are with the Department of Physics and Astronomy, University of Utah, Salt Lake City, UT 84112 USA (e-mail: thaddee@physics.utah.edu; dbevans@ucsd.edu; rogachev@physics.utah.edu).

S. Li is with Plextronics, Inc., Pittsburgh, PA 15238 USA (e-mail: sli@plextronics.com).

Color versions of one or more of the figures in this paper are available online at http://ieeexplore.ieee.org.

Digital Object Identifier 10.1109/TED.2014.2339856

The main goal of this paper is to verify the utility of the cross correlated current noise spectroscopy as a simple characterization tool that can probe some dynamical properties and thus be complementary to the dc methods. Noise spectroscopy has been used extensively in the past to study carrier transport and dynamics in inorganic devices [5]. It was employed to characterize charge transport [6] and get information on the nature of defects [7], both in semiconductor [8], [9] and magnetic devices [10]. It was also used to evaluate device overall performance [11] and reliability [12]. Compared with the wide-spread application of the noise spectroscopy for characterization of the inorganic devices, there are only few studies of their organic counterparts. Noise spectroscopy was used to investigate degradation processes in OLEDs and OSCs [13], [14], to determine a transition between the space charge limited regime and trap-filling regime in unipolar organic diodes [15], [16], and to characterize defects at the metal/organic interface in organic FETs [17] and the effect of current stress on electrical and optical performance of OLEDs [18]. In all cases, only $1/f$ component of noise spectra was accessed and analyzed.

One of the technical obstacles for the noise measurements in organic devices is the high-RC constant. High value of the resistance R comes from low-carrier mobility and high value of capacitance C comes from the thin-planar structure of a device. The high-RC constant puts a limit on the bandwidth of the voltage noise measurements and makes them not particularly useful. The current noise to some extent is free from this limitation; however, its magnitude is typically very low. The sensitivity of the current noise technique can be greatly improved using recently developed cross correlation methods described in [19], which allow for the measuring of device noise at a level much smaller than the noise on the front amplifiers. In this paper, we employ the cross correlation method to study current noise properties of OLEDs with the structure similar to what is used in display application.

II. Experiment

The studied samples were a hybrid small-molecule phosphorescent OLED composed of the following layers: ITO/AQ1200/NPB(30 nm)/NPB:rphq(20 nm)/Balq(10 nm)/Bphen:$CsCO_3$(45 nm)/Al(100 nm). ITO is indium-tin oxide and AQ1200 is solution processed hole-injection layer. Emitting layer is NPB host doped with the phosphorescent dye Irphq, sandwiched between the electron (Bphen:$CsCo_3$), and hole (NPB) transport layers. The BAlq serves as a buffer layer

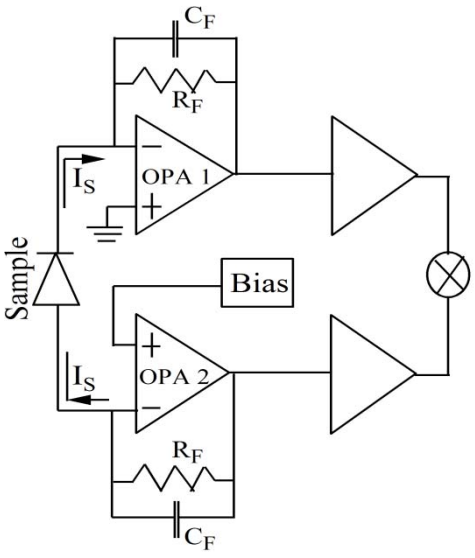

Fig. 1. Schematic view of the circuit used for current noise measurements with the cross correlation technique.

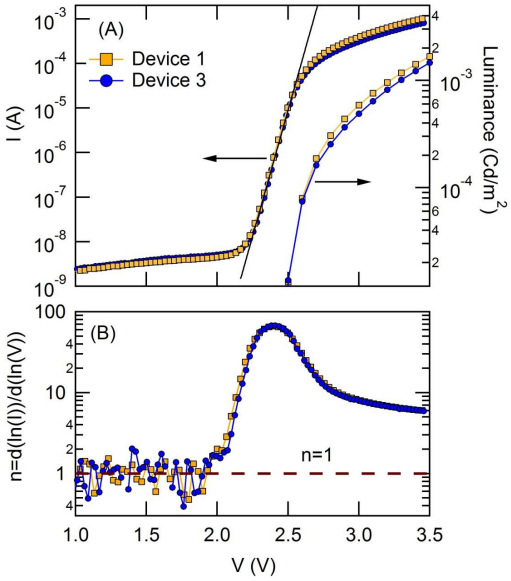

Fig. 2. (A) Current vs. voltage characteristics (left axis) for two OLEDs; luminance versus voltage for the same devices (right axis), both shown on log-liner scale. The solid line is a fit to an exponential dependence given by (1). (B) Voltage dependence of the power coefficient n for the same devices.

on cathode side. The devices were covered with a cavity glass and a getter to protect them against oxidation; the area of the devices was 9 mm^2.

Current noise measurements were performed at room temperature using a home-built apparatus. The principles of measurements are the same as in [19]. The schematic view of the circuit is shown in Fig. 1. The noise signal from a device under investigation is fed into inverting inputs of two operational amplifiers (OPA 1 and OPA 2) that convert current noise into a voltage signal. Then, the signal in each channel is amplified by OPA in the second stage. To eliminate aliases the signal passes through a low-pass filter (not shown in the figure) with a bandwidth cutoff of 300 kHz. The signals from two channels are then simultaneously read by a data-acquisition card and the cross correlation is performed. A dc voltage from a function generator was used to bias the device via a heavily filtered line.

III. Results and Discussion

The $I(V)$ characteristics and luminance curves are shown in Fig. 2(A). The latter indicates that light was detected for bias voltages >2.5 V. We also observed that the luminance depends linearly on current (Fig. 4). In semiconductor devices with injected carriers $I(V)$ characteristics often take the form $I \propto V^n$, where the power n can help to uncover a transport mechanism occurring in a given bias range. The power n can be directly calculated using the formula $n = d(Ln(I))/d(Ln(V))$. The dependence of n on bias voltage is shown in Fig. 2(B). The regime with $n = 1$ at low biases corresponds to the Ohmic conduction. It is common in organic devices and occurs because of the presence of conduction electrons and holes excited from various defects and impurities in an organic material. In the range of 2.1–2.4 V, the power index n increases linearly with voltage, which corresponds to an exponential increase of the current. This exponential increase is also evident from the $I(V)$ curve on log-linear scale between 2.2 and 2.5 V. We fit the data in this range to a standard equation for a diode

$$I(V) = I_0 \exp\left(\frac{V - V_B}{Q V_T}\right) \tag{1}$$

where $V_B = 2$ V is a fixed parameter corresponding to the built-in potential and $V_T = k_B T/e = 25.85$ meV is the thermal voltage at a temperature of 300 K. The fitting parameter I_0 was $I_0 \approx 2.3 \times 10^{-12}$ A and the ideality factor $Q \approx 1.5$. The fitting line is shown in Fig. 2, it is extended beyond the 2.2–2.5 V range for clarity. Good quantitative agreement with the diode equation and reasonable value of Q suggest that the current in this regime is injection limited and is likely controlled by the thermionic emission over a Schottky barrier formed at metal/organic interface.

Above 2.5 V, the power index sharply drops to the value of $n \approx 6$–7. This behavior can be related to the regime where the current is still controlled by injection across an electrode, but injection itself is limited by slow carrier mobility at the immediate proximity to organic/metal interface [20], [21]; this regime was reproduced in numerical modeling [22]. We observed similar evolution of the power index in polymer-based bipolar OLEDs displaying organic magnetoresistance effect [23], [24].

Fig. 3 shows the current noise spectral density as function of frequency for the two devices. The typical time of data accumulation was about 3–5 h for low-bias voltages, $V_b < 2.4$ V, and about 1 h for higher biases. The feedback resistor was 20 kΩ and feedback capacitor was 2 pF. The current cross correlation method does not completely eliminate the noise coming from the measurement setup. Assuming that the OPAs in the first stage are identical and ideal (that is they follow the OPAs golden rules [25]) and the device under test is represented by a resistor R_D and a capacitor C_D connected

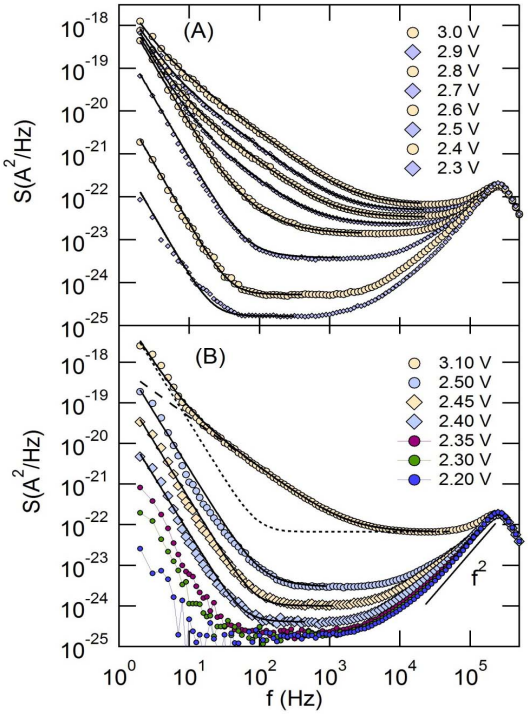

Fig. 3. (A) Current noise spectra of device 1 and (B) device 3 at indicated bias voltages. Solid lines represent the theoretical fits of the experimental data to (3). In (B) for the data at bias voltage 3.1 V, the dotted line gives the fit with the parameter S_2 set to zero and the dashed line gives the fit with the parameter S_3 set to zero.

in parallel, the residual noise is given by

$$S_{\mathrm{IR}} = e_n^2\left(\frac{1}{R_D}\left(\frac{1}{R_D}+\frac{1}{R_F}\right)\right)+e_n^2\omega^2(C_D+C_i+C_S)^2 \quad (2)$$

where e_n^2 is the input voltage noise of the OPA, C_i is the input capacitance of OPA, C_S is the stray capacitance, and R_F is the resistance of the feedback. In our case, $C_D \gg C_i, C_S$.

We found that our data are qualitatively consistent with (2). In particular, at high frequencies the noise data follow expected ω^2 dependence (the cutoff at 200 kHz is due to antialiasing filters). However, we also found that the coefficient in front of ω^2 dependence was not equal to $e_n^2C_D^2$; in addition, its magnitude increased with increasing feedback resistance R_F. The same behavior was detected for test samples composed of a resistor and capacitor. From Fig. 3(B), one can also notice that the noise data for bias voltages 2.2, 2.3, and 2.35 V are flat and overlap in the frequency range 40–1000 Hz despite the fact that the resistance of the diode R_D decreases by factor of 100 in this range. This is not what is expected from the first term in (2). Thus, the high-frequency ω^2 dependence and low-flat noise floor set the boundaries (that depends on R_F) on noise measurements with our setup. Numerous measurements of test samples verified that within this window the noise data can be accurately determined.

The noise spectra indicate very similar variation in both devices. At biases $V_b \geq 2.4$ V, the noise power density S_I has clearly identifiable flat section that shrinks and shifts to higher frequencies with increasing bias. We found that for both devices, at all biases, the noise data can be fitted by an

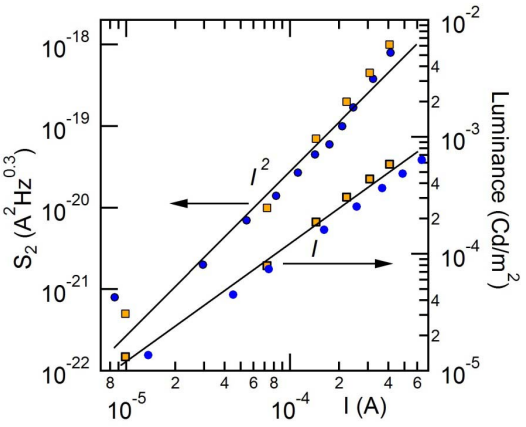

Fig. 4. Left axis: fitting parameter S_2 as a function of the current across the device. Right axis: luminance as function of current across the device. Solid lines indicate $\propto I$ and $\propto I^2$ functional dependences.

empirical expression

$$S_I = S_1 + \frac{S_2}{f^{1.3}} + \frac{S_3}{f^{2.8}} \quad (3)$$

where S_1, S_2, and S_3 are adjustable parameters. The fit to this expression is shown in the figure with solid lines. To emphasize that two frequency-dependent terms are needed, we show in Fig. 3(B), the noise data at $V = 3.1$ V alongside with two extra curves, a dotted with fitting parameter $S_2 = 0$, and dashed with fitting parameter $S_3 = 0$.

The luminance, L, of the devices, as shown in Fig. 4, is proportional to the current ($L \propto I$). From analyses of the data we found that the luminance as well as the term S_2 becomes zero below 2.5 V. This concurrent behavior suggests that term S_2 can be assigned to a recombination process related to the light emission (the appearance of $1/f$ noise term for this process is not uncommon and was detected in optical noise spectra of inorganic LEDs [26], [27]). In phosphorescent OLED, based on Ir(phq)$_3$-doped NPB host, the light emission occurs via several mechanisms. In the first mechanism, singlet and triplet excited states are formed in the host and the triplet emission occurs via energy transfer from the host to the phosphorescent dopant. A second, more efficient mechanism is the direct electron injection to the phosphorescent dopant at high-doping concentration and subsequent formation of triplet exciton directly on phosphorescent dopant. A third mechanism is a result of a capture of an electron from a host by a phosphorescent dopant with consequent recombination with a trapped hole on the same dopant. The last two charge-trapping mechanisms can be classified as a monomolecular recombination process mediated by recombination center. For such a process, the carriers' lifetime typically does not depend on carrier concentration. The term S_2 increases in magnitude with increasing current in the devices, but there is no shift to higher frequency or appearance of any generation-recombination bump (with a bias-dependent position). This gives further support to our assignment of the S_2 term to the monomolecular recombination mediated by the phosphorescent dopant molecules. In addition, as it is shown in Fig. 4, the magnitude of the term grows as a square of a current across

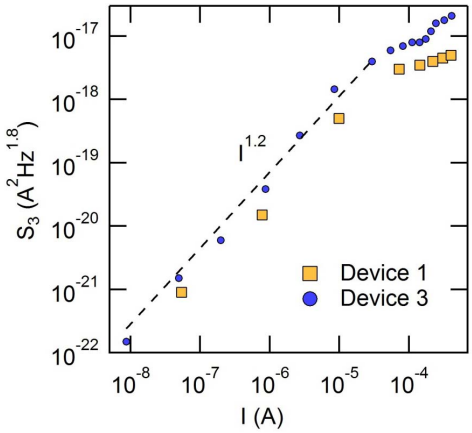

Fig. 5. Fitting coefficient S_3 as function of the current in two devices. Dashed line indicates a functional dependence $S_3 \propto I^{1.2}$.

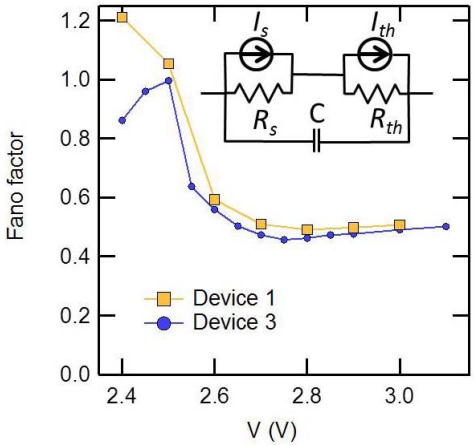

Fig. 6. Fano factor of the devices versus voltage. Inset: possible equivalent noise circuit diagram representing the diodes.

the device, $S_2 \propto I^2$, which is often interpreted as a behavior in which current probes existing defects in a system [28].

The second frequency-dependent term, S_3, is detectable at bias voltages $V_b < 2.5$ V, where there is no light emission. In this range, the parameter S_3 varies as $S_3 \propto I^{1.2}$ (Fig. 5). The functional dependence $S_I \propto I$ was observed in low-bias regime of inorganic semiconductor diodes. While an exact physical process responsible for this contribution is not yet unambiquously established, it was related to the barrier resistance [26]. Thus, the observation of $S_I \propto I^{\beta}$ behavior with $\beta \approx 1.3$ in platinum silicide Schottky barrier diodes was attributed to inhomogeneity of the barrier height at the PtSi/n-Si interface caused by grain boundaries in silicide material [29]. Similar inhomogeneities might occur at metal/organic and/or organic/organic interfaces of phosporescent diodes reported here.

The cross correlation method allows to resolve frequency-independent part of the noise. Such contribution can be generated by thermal and shot noises. As it was pointed earlier, the flat sections of the noise data at 2.2 V. The 2.3 and 2.35 V coincide and set the noise floor of our measurement apparatus at the level $S_{\rm FL} = 1.9 \times 10^{-25}$ A^2/Hz. The frequency-independent noise contribution was determined as $S_{\rm exp} = S_1 - S_{\rm FL}$, where the parameter S_1 is obtained from fitting. In the inset of Fig. 6, we display a possible equivalent circuit diagram representing the diodes. The diagram includes a shot noise generator, I_S, and a thermal noise generator, $I_{\rm th}$. Physically, the shot noise can be generated by thermionic emission or tunneling across a Schottky barrier at metal/organic interface. In addition, as in the case of inorganic diodes [30], the shot noise can be generated by electron-hole recombination. The thermal noise stems from the hopping transport of carriers across the device. Even for this simplified equivalent model, resistors of two noise sources, R_S and $R_{\rm th}$, appear in series and cannot be determined from our data. Therefore, for the analysis we first assume that $R_S \gg R_{\rm th}$, which is equivalent of saying that $S_{\rm exp}$ is mostly generated by the shot noise.

The shot noise is given by the well-known expression $S_S = F2eI$, where F is the Fano factor characterizing shot noise suppression. The Fano factor computed as $F = S_{\rm exp}/(2eI)$ is shown in Fig. 6. Its values in the bias regime 2.4–2.5 V appear to be closed to one; however, this conclusion depends on the assumption that $R_S \gg R_{\rm th}$. A complication here is that values of the thermal noise computed with formula $S_{\rm th} = 4k_BT/R_{\rm tot}$, where $R_{\rm tot}$ is total differential resistance of the diode, appear to be close to the values of $S_{\rm exp}$. Nevertheless, from physical grounds we believe that the assumption $R_S \gg R_{\rm th}$ (or equivalently, $R_S \approx R_{\rm tot}$) should be applicable here. Let us explain our reasoning. From the $I(V)$ curve, one can observe that points in the range 2.4–2.5 V appear at the end of the exponential $I(V)$ dependence. The exponential $I(V)$ is not expected for any bulk transport process in unipolar or bipolar insulators with injected carriers [31]. Very likely, it corresponds to a thermionic emission across a Schottky barrier formed at metal/organic interface. In this case, the resistance of the whole device is dominated by the resistance of the barrier and full-scale ($F = 1$) shot noise is expected. It is claimed that for such strongly nonequilibrium process, one must not associate any thermal noise with the differential resistance of the barrier [32]. Therefore, the assumption $R_S \gg R_{\rm th}$ is physically reasonable and gives consistent interpretation of both current and noise variation in this bias regime.

The Fano factor is approximately constant and equal to 0.5 in the bias range 2.6–3.1 V. In this range, one can relax the assumption $R_S \gg R_{\rm th}$, since an estimated thermal noise is about four times smaller than $S_{\rm exp}$. Two signatures of $S_{\rm exp}$, linear dependence on current and independence of frequency, indicate that this term represents shot noise. It is very unlikely that the shot noise in this regime is generated by a barrier at a metal/organic interface. The appearance of the Fano factor $F = 0.5$ within this barrier mechanism requires that the barrier differential resistance is $R_{\rm BAR} = R_S \approx 0.5R_{\rm tot}$, which in turn means that half of the bias voltage drops across the barrier. If this is the case, from the extrapolation of the exponential dependence characterizing the transport across the barrier and shown in Fig. 2 by a solid line, we would expect the current in the device to be several orders of magnitude larger than what is observed experimentally. The transport in the device at $V > 2.6$ V is limited by the bulk resistance of the device, and therefore, the shot noise in this regime also has a bulk origin.

One of the possibilities is that the shot noise is produced by electron-hole recombination process responsible for the

light emission, because this process results in a random instantaneous removal of carriers [30]. Another possibility is that the shot noise comes from the hopping transport process itself. An elementary step of this process is a jump with length of 1–2 nm over a potential barrier separating two localized states in an organic material. The jump itself is a discrete event that is expected to generate a full-scale shot noise. The situation is more complex when sequential hops are considered. In a simple 1-D model in which a carrier tunnels through N equivalent potential barriers, the Fano factor is suppressed as $F = 1/N$ [33]. However, in a disordered chain, the resistance is dominated by a small number of so-called hard hops and the shot noise can increase significantly [33]. This phenomenon was recently observed in the variable-hopping regime of carriers confined in a p-type SiGe quantum well [34]. The average hopping length of an electron was 80 nm at $T = 4$ K. Yet for a sample of length 2 μm, the shot noise with $F = 0.5$ was observed. The large Fano factor was consistent with the estimated distance between hard hops suggesting that the shot noise is generated at one or two electron transitions that limit conductance across a particular hopping chain. Disordered nature of organic materials used in OLEDs makes the appearance of such percolating chains very plausible. Further experiments and detailed theoretical analysis are needed to confirm this mechanism. However, if its presence is indeed confirmed, the noise measurements will emerge as a very valuable tool for detailed characterization of electron transport in organic materials, their uniformity and degradation processes.

IV. Conclusion

In summary, we have employed the cross correlated method for the measurements of the current noise in phosphorescent OLEDs. This method allowed us to access and to characterize several phenomena in these devices; it complimented the dc transport and electroluminescence measurements well. The most important result is the observation of shot noise in the regime where the transport in the devices is limited by the bulk conduction in the OLEDs.

Acknowledgment

The authors would like to thank M. Raikh for his valuable comments and discussions.

References

[1] S. H. Park *et al.*, "Bulk heterojunction solar cell with internal quantum efficiency approaching 100 %," *Nature Photon.*, vol. 3, pp. 297–302, Apr. 2009.

[2] M. A. Green, K. Emry, Y. Hishikawa, W. Warta, and E. D. Dunlop, "Solar cell efficiency tables (version 39)," *Progr. Photovolt., Res. Appl.*, vol. 20, no. 1, pp. 12–20, 2012.

[3] J. Shinar and R. Shinar, "Organic light-emitting devices (OLEDs) and OLED-based chemical and biological sensors: An overview," *J. Phys. D, Appl. Phys.*, vol. 41, no. 13, p. 133001, 2008.

[4] W. Brütting, J. Frischeisen, T. D. Schmidt, B. J. Scholz, and C. Mayr, "Device efficiency of organic light-emitting diodes: Progress by improved light outcoupling," *Phys. Status Solidi A*, vol. 210, no. 1, pp. 44–65, 2013.

[5] K. Tanaka, A. Higashi, H. Yuri, R. Masuyama, Y. K. Adoya, and M. Yamanishi, "Wideband sub-Poissonian light generation in light-emitting diodes incorporating a heavily-doped active region," *Appl. Phys. Lett.*, vol. 81, no. 18, pp. 3317–3319, 2002.

[6] G. Bosman, "Charge transport and device parameters from noise measurements," *IEEE Trans. Electron Devices*, vol. 41, no. 11, pp. 2198–2204, Nov. 1994.

[7] B. K. Jones, "Low-frequency noise spectroscopy," *IEEE Trans. Electron Devices*, vol. 41, no. 11, pp. 2188–2197, Nov. 1994.

[8] E. Simoen, A. Mercha, L. Pantisano, C. Claeys, and E. Young, "Low-frequency noise behavior of SiO_2–HfO_2 dual-layer gate dielectric nMOSFETs with different interfacial oxide thickness," *IEEE Trans. Electron Devices*, vol. 51, no. 5, pp. 780–784, May 2004.

[9] E. G. Ioannidis, A. Tsormpatzoglou, D. H. Tassis, C. A. Dimitriadis, F. Templeir, and G. Kamarinos, "Characterization of traps in the gate dielectric of amorphous and nanocrystalline silicon thin-film transistors by $1/f$ noise," *J. Appl. Phys.*, vol. 108, no. 10, pp. 106103-1–106103-3, 2010.

[10] K. B. Klaassen, "Electrical low-frequency noise in tunneling magnetoresitive heads: Phenomena and origins," *IEEE Trans. Magn.*, vol. 43, no. 2, pp. 663–670, Feb. 2007.

[11] G. Niu, "Noise in SiGe HBT RF technology: Physics, modeling, and circuit implications," *Proc. IEEE*, vol. 93, no. 9, pp. 1583–1597, Sep. 2005.

[12] S. Mohammadi, D. Pavlidis, and B. Bayraktarogly, "Relation between low-frequency noise and long-term reliability of single AlGaAs/GaAs power HBTs," *IEEE Trans. Electron Devices*, vol. 47, no. 4, pp. 677–686, Apr. 2000.

[13] G. Ferrari *et al.*, "Current noise spectroscopy on mLPPP based organic light emitting diodes," *Organic Electron.*, vol. 3, no. 1, pp. 33–42, 2002.

[14] L. Ke, X. Y. Zhao, R. S. Kumar, and S. J. Chua, "Low-frequency noise measurement and analysis in organic light-emitting diodes," *IEEE Electron Device Lett.*, vol. 27, no. 7, pp. 555–557, Jul. 2006.

[15] A. Carbone, B. K. Kotowska, and D. Kotowski, "Space-charge-limited fluctuations in organic semiconductors," *Phys. Rev. Lett.*, vol. 95, no. 23, p. 236601, 2005.

[16] A. Carbone, C. Pennetta, and L. Reggiani, "Trapping-detrapping fluctuations in organic space-charge layers," *Appl. Phys. Lett.*, vol. 95, no. 23, p. 233303, 2009.

[17] J. Xu *et al.*, "Extraction of low-frequency noise in contact resistance of organic field-effect transistors," *Appl. Phys. Lett.*, vol. 97, no. 3, pp. 033503-1–033503-3, 2010.

[18] K. Lin, L. S. Cheng, A. Ramam, and C. S. Jin, "Correlation analysis of electrical and optical low frequency fluctuation in organic device degradation," *J. Appl. Phys.*, vol. 105, no. 6, pp. 064504-1–064504-7, 2009.

[19] M. Sampietro, L. Fasoli, and G. Ferrari, "Spectrum analyzer with noise reduction by cross-correlation technique on two channels," *Rev. Sci. Instrum.*, vol. 70, no. 5, pp. 2520–2525, 1999.

[20] M. A. Baldo and S. R. Forrest, "Interface-limited injection in amorphous organic semiconductors," *Phys. Rev. B*, vol. 64, no. 8, p. 085201, 2001.

[21] J. C. Scott and G. G. Molliaras, "Charge injection and recombination at the metal—Organic interface," *Chem. Phys. Lett.*, vol. 299, no. 2, pp. 115–119, 1999.

[22] E. Tutis, M. N. Bussac, B. Masenelli, M. Carrad, and L. Zuppiroli, "Numerical model for organic light-emitting diodes," *J. Appl. Phys.*, vol. 89, no. 1, pp. 430–439, 2001.

[23] T. K. Djidjou, T. Basel, and A. Rogachev, "Admittance spectroscopy study of polymer diodes in small magnetic fields," *J. Appl. Phys.*, vol. 112, no. 2, p. 024511, 2012.

[24] T. K. Djidjou, T. Basel, and A. Rogachev, "Magnetic-field dependent differential capacitance of polymer diodes," *Appl. Phys. Lett.*, vol. 101, no. 9, p. 093303, 2012.

[25] P. Horowitz and W. Hill, *The Art of Electronics*. Cambridge, U.K.: Cambridge Univ. Press, 2001, p. 94.

[26] S. Sawyer *et al.*, "Current and optical noise of GaN/AlGaN light emitting diodes," *J. Appl. Phys.*, vol. 100, no. 3, pp. 034504-1–034504-5, 2006.

[27] S. L. Rumyantsev *et al.*, "Low-frequency noise of GaN-based ultraviolet light-emitting diodes," *J. Appl. Phys.*, vol. 97, no. 12, pp. 123107-1–123107-5, 2005.

[28] F. N. Hooge, "$1/f$ noise sources," *IEEE Trans. Electron Devices*, vol. 41, no. 11, pp. 1926–1935, Nov. 1994.

[29] S. Papatzika, N. A. Hastas, C. T. Angelis, C. A. Dimitriadis, G. Kamarinos, and J. I. Lee, "Investigation of noise sources in platinum silicide Schottky barrier diodes," *Appl. Phys. Lett.*, vol. 80, no. 8, pp. 1468–1470, 2002.

[30] P. J. Edwards, "Sub-Poissonian recombination noise in macroscopic and mesoscopic semiconductor junctions," in *Noise and Fluctuations Control in Electronic Devices*. Stevenson Ranch, CA, USA: American Scientific Publishers, 2002.
[31] K. C. Kao and W. Hwang, *Electrical Transport in Solids*. New York, NY, USA: Pergamon, 1981.
[32] M. Trippe, G. Bosman, and A. Van Der Ziel, "Transit-time effects in the noise of Schottky-barrier diodes," *IEEE Trans. Microw. Theory Techn.*, vol. 34, no. 11, pp. 1183–1192, Nov. 1986.
[33] A. N. Korotkov and K. K. Likharev, "Shot noise suppression at one-dimensional hopping," *Phys. Rev. B*, vol. 61, no. 23, pp. 15975–15987, 2000.
[34] V. V. Kuznetsov, E. E. Mendez, X. Zuo, G. L. Snider, and E. T. Croke, "Partially suppressed shot noise in hopping conduction: Observation in SiGe quantum wells," *Phys. Rev. Lett.*, vol. 85, no. 2, pp. 397–400, 2000.

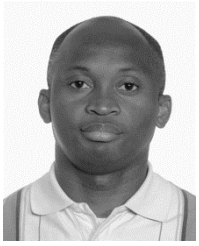

Thaddee Kamdem Djidjou received the Ph.D. degree in experimental condensed matter physics from the University of Utah, Salt Lake City, UT, USA, in 2013.

He is currently a Research Assistant with the Department of Physics and Astronomy, University of Utah. His current research interests include nanoscience and nanaotechnology, and the charge transport in organic semiconductor devices.

Dieter Alexander Bevans received the B.S. degree in physics from the University of Utah, Salt Lake City, UT, USA, in 2012, and the M.S. degree from the Scripps Institution of Oceanography, La Jolla, CA, USA, in 2014, where he is currently pursuing the Ph.D. degree.

His current research interests include deep sea ambient noise, deep sea instrumentation, and low-frequency noise in a shallow Pekeris waveguide.

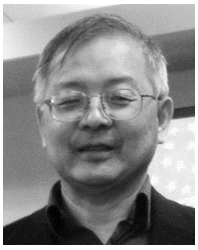

Sergey Li received the Ph.D. degree in solid-state physics from the Department of Thermal Physics, Uzbekistan Academy of Sciences, Toshkent, Uzbekistan, in 1996.

He joined Plextronics, Inc., Pittsburgh, PA, USA, in 2006, as a Senior Scientist. His current research interests include the hole-injecting and hole-transport materials and its applications in organic light-emitting diodes for display and lighting industry.

Andrey Rogachev received the Ph.D. degree in material science from Nagoya University, Nagoya, Japan, in 2000.

He joined the Department of Physics and Astronomy at the University of Utah, Salt Lake City, UT, USA, in 2006, where he is currently an Associate Professor. His current research interests include electron transport in disordered systems, microscopic physics, nanoscience and nanotechnology, and physics of low-dimensional superconducting systems.